

M. Riva, D. Mazon, R. Felton, X. Litaudon, G. Tresset, A. Becoulet, J.M. Chareau,
S. Dalley, S. Dorling, E. Joffrin, D. Moreau and JET EFDA Contributors

Towards Real Time Control of the Internal Transport Barriers on JET

Towards Real Time Control of the Internal Transport Barriers on JET

M. Riva¹, D. Mazon², R. Felton³, X. Litaudon², G. Tresset², A. Becoulet²,
J.M. Chareau², S. Dalley³, S. Dorling³, E. Joffrin², D. Moreau²
and JET EFDA Contributors

¹*Associazione Euratom-ENEA sulla Fusione, C.R. Frascati, 00044 Frascati Italy,
presently seconded at JET/UKAEA under JOC contract.*

²*Association Euratom-CEA, CEA Cadarache, F-13108, St Paul lez Durance, France* ³*EURATOM/*

³*EURATOM/UKAEA Fusion Association, Culham Science Centre, Abingdon, OX14 3DB, UK*

** See annex of J. Pamela et al, "Overview of Recent JET Results and Future Perspectives",
Fusion Energy 2000 (Proc. 18th Int. Conf. Sorrento, 2000), IAEA, Vienna (2001).*

Preprint of Paper to be submitted for publication in Proceedings of the
19th IEEE/NPSS Symposium on Fusion Engineering
(Atlantic City, New Jersey, USA 22-25 January 2002)

“This document is intended for publication in the open literature. It is made available on the understanding that it may not be further circulated and extracts or references may not be published prior to publication of the original when applicable, or without the consent of the Publications Officer, EFDA, Culham Science Centre, Abingdon, Oxon, OX14 3DB, UK.”

“Enquiries about Copyright and reproduction should be addressed to the Publications Officer, EFDA, Culham Science Centre, Abingdon, Oxon, OX14 3DB, UK.”

ABSTRACT.

Recently a local criterion characterising the emergence and space-time evolution of Internal Transport Barriers (ITB) has been proposed and extensively validated on the large JET database [1]. It was shown that a dimensionless local parameter, $\rho_{Te}^* = \rho_S / L_{Te}$ characterises with a low computational cost the typical ITB features such as the emergence time, location, collapse time and dynamics [ρ_S is the local Larmor radius and L_{Te} is the temperature gradient scale length $L_{Te} = -T_e (\partial T_e / \partial R)$]. We report on the recent implementation of the calculation of the ITB criterion together with the associated feedback algorithms in the real time system of JET. The system purpose is to acquire all the analogue channels of the high space resolution electron temperature ECE diagnostic (heterodyne radiometer) and to calculate in real time the relevant ITB parameters which are used for the control: the maximum value of the dimensionless local temperature gradient, the ITB radius and width, the core and volume averaged electron temperature.

1. HARDWARE DESCRIPTION

The general real-time system is depicted in Fig. 1. It is based on a VME crate, hosting a VPLS Crate Service Module, a PowerPC CPU and two multichannel data acquisition boards.

The system acquires 48 analogue channels from the ECE diagnostic CAMAC system at 1 KHz sampling frequency. The system uses the 1KHz VPLS hardware interrupt as trigger for this sampling. These operate as mailbox interrupts to the Power PC. The second hardware signal used is the PRE signal, coming from the JET timing and trigger system (CTTS).

The PowerPC processor does all the pre-processing and elaboration. This is a Motorola MVME2432 VME board with 64 Mbytes of RAM, 350MHz clock. It is equipped with an ATM PMC PCI board, to allow future expansion to the Real Time Signal Server (RTSS) without using analogue cables. The Crate Service module is a standard JET CPU board. It accepts a fiber-optic link from CTTS and produces the hardware signals as interrupts. As a future development we think to upgrade the CPU to allow the acquisition of more channel (96) maintaining the overall cycle time below one millisecond (presently the cycle time is about 700 microseconds).

The ADC/DACs are two acquisition boards. They are PENTLAND MPV956B analogue I/O boards that have 12-bit 320KHz sampling rate ADC. The channels can be 32 single ended or 16 differential (we use the single ended) and they have also 8 12-bit DAC, that we use to produce the analogue outputs. The RTSS collects and sends signals across the JET facilities in real time and the Real Time Central Controller (RTCC) performs the control actions on the JET machine using the heating systems [2,3].

2. SOFTWARE DESCRIPTION

The code development was done under vxWorks real time operating system, which is widely used at JET. The software architecture is described by Fig 2.

We can see that 4 processes plus 2 interrupt processes and 4 semaphores (Restart, Dbg, End, and Hist) form the software system. The Start process is the interface with the JET GAP/countdown

system, and it waits until a queue message arrives. This message contains all the parameter to start a new calculation phase. Then it creates (spawn) the goITB process. The go ITB process waits the JET PRE hardware signal, which means that a new shot is arriving. Then it spawns the two processes Hist and End, and waits on the Dbg semaphore to be taken. When the End process releases the Dbg semaphore, all the data are ready to be stored in the JET post Pulse File data base (JPF) system by the GAP process.

The Hist process is the system core. It acquires the ECE radiometer signals, calibrates them, calculates the ITB parameters and produces the outputs. When the shot is finished, it releases the End semaphore. The End process performs the finishing procedures, and releases the Dbg semaphore, allowing the system to return in an idle state, waiting the next shot.

3. THE ALGORITHM

The algorithm, is a derivation and a generalisation of the original algorithm presented in [1]. The main purpose of the algorithm is to calculate the a dimensional parameter

$$\rho_{Te}^*(R,t) = -\frac{1}{Z} \left(\frac{Am_p}{e} \right)^{1/2} \frac{T_e^{1/2}}{B_T} \frac{1}{T_e} \frac{\partial T_e}{\partial R}$$

With:

- R the major radius,
- Z the charge number (Z=1 in our case),
- A the Atomic plasma species (A=2 for deuterium plasma),
- m_p is the proton mass,
- e is the electric charge,
- B_T is the toroidal field in tesla.

Each acquired measure is related to the electron temperature at a given radius. So the ordered set of all the couples (radius, temperature) form a graphic called “Electron Temperature profile”. The following Fig 3 shows an example of the profiles, with an example of ITB, which is a break in the slope of T_e .

During the elaboration phase, the algorithm first calculates the radius and the vacuum field for each channel interpolating the RCs and the BVAC at that time. The RCs are the radii of the ECE line of sight projected on the magnetic axis and we have stored their values in memory in the initialisation phase. The only limitation in this version is that we must use the RC and the BVAC values related to a previous “similar” JET shot. Similar means essentially the same current and the same magnetic field. In the future we are thinking to use a real time value of BVAC, and also a real time calculation of the RCs.

Now we have, in real time, all the quantities to calculate the electron temperatures profiles from the acquired radiometer signals. The formula used for the calibration is:

$$Te_i = (Chan_i - Baseline_i) CAL_i$$

Where Te_p , is the electron temperature, $Chan_i$ is the acquired channel, $Baseline_i$ is the baseline calculated in the pre-plasma phase and CAL_i is the calibration factor calculated in the initialisation phase. The Baseline is essentially an offset to subtract to each measure, and it is calculated in a parametric temporal range before the plasma.

The physical quantities available in real time and calculated in the algorithm are explained and shown in the following figures (from Fig 4 to Fig 8, relatives to the Pulse No: 53698):

The Central Electron temperature Te_0 is the temperature with the closest radius to R_CORE in the outer side of the plasma. R_CORE is a constant and normally is 3.0 meters.

The Average electron temperature $\langle Te \rangle$ is defined by:

$$\langle Te \rangle = \frac{\sum_k (RC_k - R_CORE) Te_i}{\sum_k (RC_k - R_CORE)}$$

with $R_CORE \leq RC_k \leq R_EDGE$ (default 3.9m)

The ρ_{Te}^* is the normalised electron temperature gradient. According with [1], the ITB is detected when $\rho_{Te}^* \geq THRESHOLD$ Where THRESHOLD is the constant 0.014. This latest value has been determined for JET pulses from a large database.

The Major radius R_{ITB} is associated with the ρ_{Te}^* . If there is no ITB then $R_{ITB} = NO_ITB$. The algorithm starts to calculate the Te_0 and $\langle Te \rangle$. Then it calculates the normalised electron temperature gradient for each the 48 points applying the three point's rule: if there are 3 consecutive points beyond the threshold, the criterion is fixed as the maximum between the three. The procedure continues 3 by 3 points for all the 48 points until we found the maximum between the maxima. At this point, the ρ_{Te}^* is this maximum. Furthermore only a radial window from R_MIN=3.2 meters to R_MAX=3.7 meters is considered so as to avoid the irrelevant measurement and a possible edge barrier.

One of the limitations of the original algorithm is that it is not capable of calculating a valid criterion when there are not three good consecutive points. This is unacceptable if we are looking for an algorithm useful in a control environment. We would like also an algorithm that doesn't have jumps when the criterion passes the threshold. With this in mind, we modified the original algorithm in the following way.

If there exist three consecutive points above the threshold, the criterion is calculated in the usual way. If not, this leads to three cases:

If the number is zero, this means that we stay below the threshold, so we choose the maximum between the three points. In case of one, we have two possibilities (depending on an internal parameter in the code). In one case we choose the second value of the ordered tern, in the other the maximum value. The third case means that we have 2 points above the threshold. This is the best approximation to the original algorithm and we choose the maximum value of the tern. When we have scanned all the 48 points (3 by 3), we choose the actual maximum. This algorithm has been used in all the C4 campaign at JET with successful results.

We added also another variant to the algorithm, the so called “follower” algorithm. In this particular case, we calculate in the usual way the criterion but, in case we lose the ITB (in the previous time slice the criterion is above the threshold and in the following it stays below), we restrict our attention to a (parametric) little range centered to the previous radius position. This holds in the situation where the ITB is still there and we lose it only for few time slices. As soon as we regain a strong ITB (i.e. three points above the threshold), the system returns in the usual way.

Several other parts were added to improve the algorithm. The most important is the ELM “catcher”. The ELM is a plasma activity that dramatically changes the shape of the electron temperature profile, only for one or two consecutive samples (its activity lasts usually less than 1 millisecond). So we added a simple algorithm that recognises if, in that time slice, there is an ELM. In that case, assuming that in one millisecond the electron temperature profile doesn’t change very much, we keep the previous profile. This leads to a smoother criterion because using the ELM disturbed profile we could have peaks in the curve which are not related to the physics of the phenomenon (the ITB).

Also it was added the possibility to use a low pass digital filter for each input, to reduce the input noise. This can be set using a parameter.

On the output side, another digital filter was added to reduce the output noise on the criterion and the radius. This is a special digital filter called a “median” filter, which is well suited for spike removal. We used in the algorithm a length 11 median filter.

During the development a new output was added, called ITB width (Fig 8). It is the width, in meters, of the ITB. In other words, it is the range around the ITB position where the threshold is exceeded. This can be used also as a visual detection of the ITB formation: when this measure is different from zero, a barrier is detected.

In the following Fig 9 we can see the elms channel during the shot #53698. Comparing Fig 6 with Fig 9 we can see the quality of the $\rho_{T_e}^*$ in presence of ELMs. From 47 to 48 seconds there are many elms. Due to the elms catcher algorithm, the $\rho_{T_e}^*$ is not affected by spikes in that range (in this shot were caught about 700 elms).

4. RESULTS ON REAL TIME ITB CONTROL

The algorithm used to control the ITB is based on the error between a target reference and the real. A PI approach has been chosen and the general formula for the control is:

$$P(t) = P_0 + G_p \Delta\rho + G_i \int_{t_0}^t \Delta\rho dt$$

Where $G_p = 10$ and $100 < G_i < 1000$ and $\Delta\rho$ is the error. The error is the difference between the reference criterion and the calculated one, using as criterion the $\rho_{T_e}^*$ or the neutron rate. The value for G_p was chosen to avoid strong power variation and the range for G_i was chosen to well integrate the time behavior of $\rho_{T_e}^*$. P_0 is the power at the initial time t_0 in MW. It can be Ion Cyclotron Resonance Heating) ICRH or the Neutral Beam (NBI).

Many controls have been done during the last experimental campaign using both heating systems as actuators [4].

We can see on Fig.10(a) an example of control with ICRH. The target reference values are achieved perfectly in a regime with $T_{i0} = T_{e0} = 7keV$.

In Fig.10(b) a double control on $\rho_{T_e}^*$ using ICRH and on the neutron rate using NBI for improving stability is presented. The values of $\rho_{T_e}^*$ and the neutron rate are maintained constant respectively at 0.025 and $0.9 \cdot 10^{16}$ neutron/s. The ITB is controlled and sustained during 7.5 s and stops with the preprogrammed power waveform.

The comparison with a not controlled shot, having the same experimental conditions [See Fig.10(b)] shows the importance of the control for stability. This shot has several collapses caused by MHD events or impurity accumulation and was close to a disruption. The effect of the double control demonstrates the possibility to control high performance regimes [5] in a steady state operation.

CONCLUSIONS

The main ITB parameters are now available at JET. The calculation of $\rho_{T_e}^*$ is robust and has been implemented and used in real time during the C4 experimental campaign. The first attempt to perform real time plasma control has been tested successfully in a variety of plasma conditions (different toroidal field and plasma currents), acting on $\rho_{T_e}^*$ or on neutron rate. New project in JET will attempt to control in real time also the ITB radius (the ITB location) and also the system will use the ATM network to distribute signals digitally without use of analogue cables.

REFERENCES

- [1]. Tresset G. & al EFDA-JET-PR(00)09.
- [2]. Q. A. King, H. E. O. Brelen, An Experimental Automatic Control Facility at JET, JET P(98)24.
- [3]. R. Felton & al, Real Time Plasma Control at JET using an ATM Network, JET-P(99)27.
- [4]. Mazon D. & al 28th EPS conference Madeira.
- [5]. Litaudon X. & al 28th EPS conference Madeira.

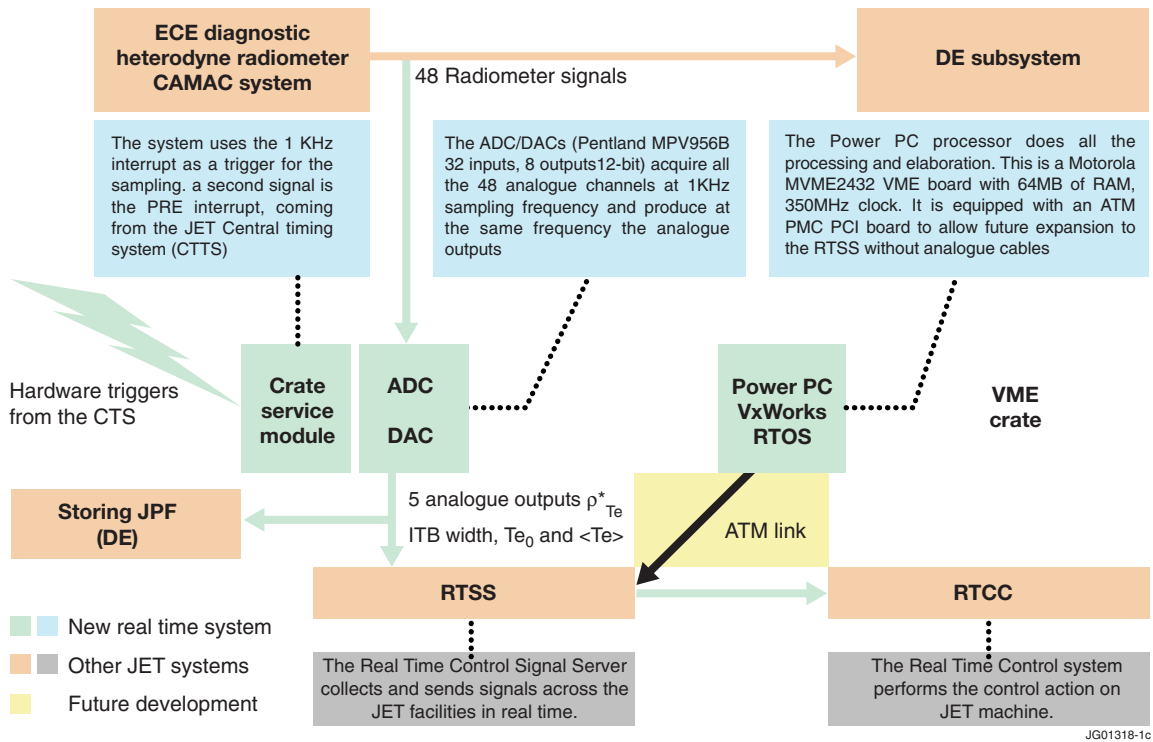


Figure 1: The General real-time system.

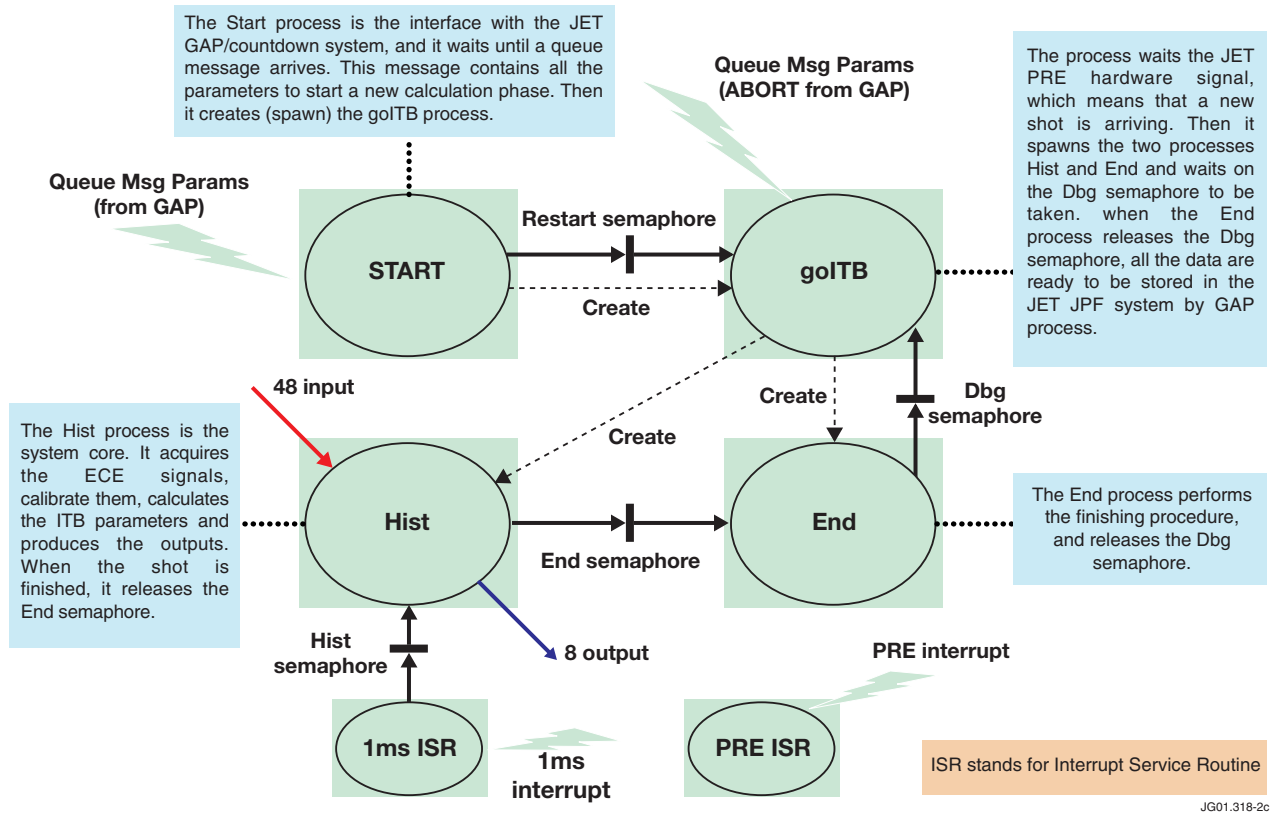


Figure 2: The software architecture system.

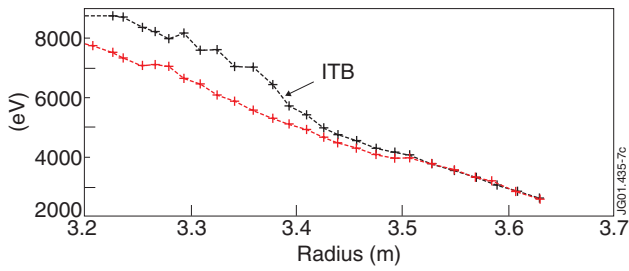


Figure 3: Pulse No: 53698. The green profile was taken at 5.2 ec and there is no ITB. The blue profile was taken at 46 sec and there is an ITB located at 3.39m.

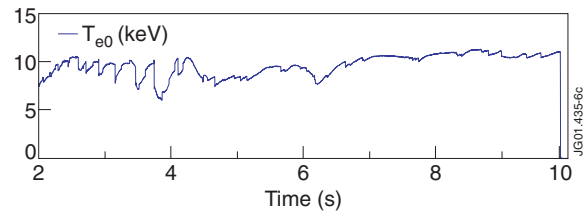


Figure 4: Central electron temperature T_{e0} .

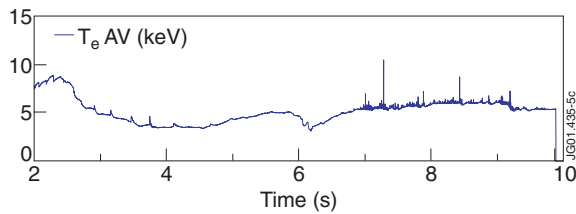


Figure 5: Average Temperature.

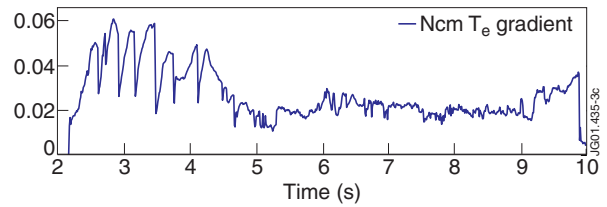


Figure 6: Normalised T_e gradient ρ^*_{Te} .

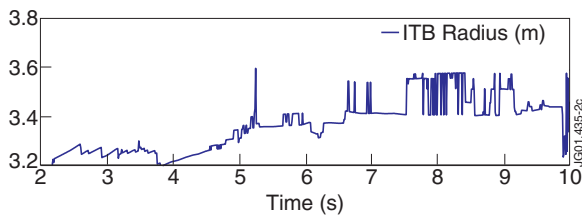


Figure 7: Radius of the ITB R_{ITB} .

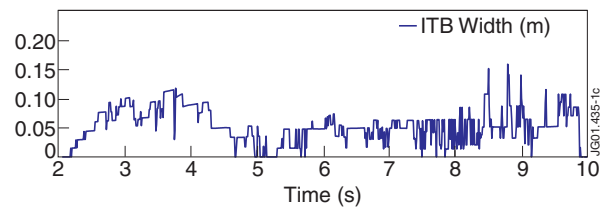


Figure 8: ITB Width.

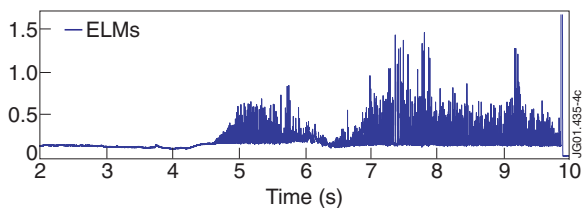


Figure 9: JET Pulse No: 53698 elms.

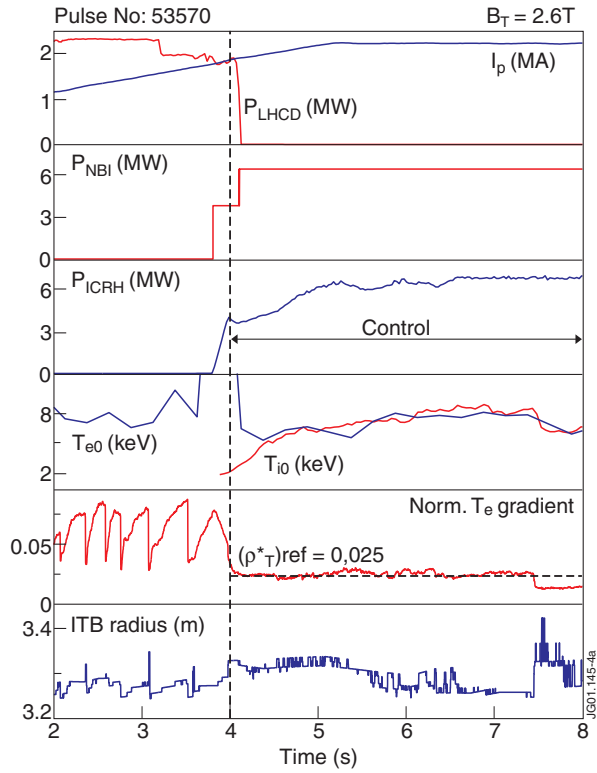


Figure 10: (a) Control with ICRH: Time evolution of LH power, plasma current, NBI, ICRH power, T_{e0} , T_{i0} , ρ_{Te}^* , ITB radius and width of the ITB (JET Pulse No: 53570). Control starts at 4 sec. And the reference value for ρ_{Te}^* is 0.025.

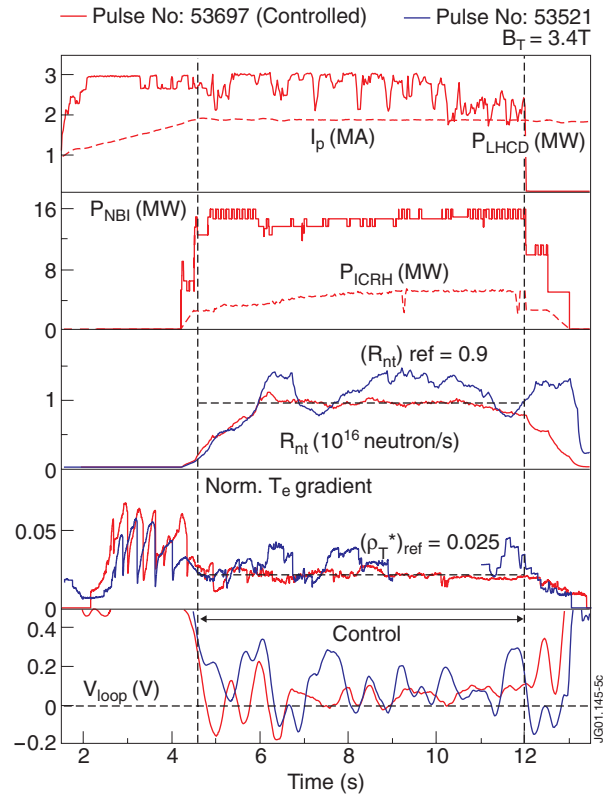


Figure 10: (b) Control with ICRH and NBI: Time evolution of LH power, plasma current, NBI, ICRH power, neutron rate, ρ_{Te}^* , loop voltage (comparison Pulse No: 53521 without control with the controlled Pulse No: 53697).